Two complementary features of humoral immune memory confer protection against the same or variant antigens

Citation: M. Van Beek, M.C. Nussenzweig, A.K. Chakraborty, Two complementary features of humoral immune memory confer protection against the same or variant antigens, Proc. Natl. Acad. Sci. U.S.A.119 (37) e2205598119.

As Published: 10.1073/pnas.2205598119

Publisher: Proceedings of the National Academy of Sciences

Persistent URL: https://hdl.handle.net/1721.1/157803

Version: Final published version: final published article, as it appeared in a journal, conference proceedings, or other formally published context

PNAS RESEARCH ARTICLE | IMMUNOLOGY AND INFLAMMATION
BIOPHYSICS AND COMPUTATIONAL BIOLOGY OPEN ACCESS

Two complementary features of humoral immune memory confer protection against the same or variant antigens

Matthew Van Beek[a], Michel C. Nussenzweig[b,c], and Arup K. Chakraborty[a,d,e,f,g,1]

Contributed by Arup K. Chakraborty; received March 30, 2022; accepted June 22, 2022; reviewed by Jason Cyster and Thierry Mora

The humoral immune response, a key arm of adaptive immunity, consists of B cells and their products. Upon infection or vaccination, B cells undergo a Darwinian evolutionary process in germinal centers (GCs), resulting in the production of antibodies and memory B cells. We developed a computational model to study how humoral memory is recalled upon reinfection or booster vaccination. We find that upon reexposure to the same antigen, affinity-dependent selective expansion of available memory B cells outside GCs (extragerminal center compartments [EGCs]) results in a rapid response made up of the best available antibodies. Memory B cells that enter secondary GCs can undergo mutation and selection to generate even more potent responses over time, enabling greater protection upon subsequent exposure to the same antigen. GCs also generate a diverse pool of B cells, some with low antigen affinity. These results are consistent with our analyses of data from humans vaccinated with two doses of a COVID-19 vaccine. Our results further show that the diversity of memory B cells generated in GCs is critically important upon exposure to a variant antigen. Clones drawn from this diverse pool that cross-react with the variant are rapidly expanded in EGCs to provide the best protection possible while new secondary GCs generate a tailored response for the new variant. Based on a simple evolutionary model, we suggest that the complementary roles of EGC and GC processes we describe may have evolved in response to complex organisms being exposed to evolving pathogen families for millennia.

affinity maturation | immune memory | antibody response | vaccine | virus

Significance

We study an important question in immunology: How is B cell–mediated immune memory recalled upon reexposure to the same or variant antigens? We find that, upon reexposure to the same antigen, high-affinity memory B cells are selectively expanded outside germinal centers (GCs) to quickly provide the best protection possible. Memory B cells also enter GCs and over time produce the highest-affinity antibodies, but GCs also generate diverse B cells, some with low antigen affinity. Upon exposure to a variant antigen, these low-affinity clones can exhibit high affinity for the variant. These clones are expanded rapidly outside the GC to confer immediate protection. Over longer times, secondary GCs produce high-affinity clones tailored for the variant antigen.

The adaptive immune system plays a critical role in protecting humans from assaults by diverse pathogens. B lymphocytes (B cells) and their antibody products constitute the humoral component of adaptive immunity. B cells express a surface receptor called the B cell receptor (BCR). V-D-J recombination generates an enormous diversity of BCRs, and most B cells in the repertoire express a distinct BCR (1). If a B cell's BCR can bind sufficiently strongly to the surface of a pathogen (antigen), such as viral spike proteins, intracellular signaling activates new gene transcription programs. Activated B cells can seed germinal centers (GCs) in lymph nodes, wherein B cells undergo a Darwinian evolutionary process called affinity maturation (2). GC B cells multiply, and because they express the activation-induced cytidine deaminase enzyme, mutations are introduced in the Ig genes of these progeny at a high rate (somatic hypermutations). The B cells then undergo selection. Their mutated Igs encode BCRs that will either lose or gain affinity to the antigen displayed on follicular dendritic cells (FDCs) in the GC. Sufficiently strong binding can result in the B cell internalizing the antigen. B cells then display antigen-derived peptides bound to major histocompatibility class II molecules, which can bind to T cell receptors expressed on T helper cells. Successful engagement results in a positive selection signal. B cells with BCR that bind more strongly to antigen are more likely to be positively selected. GC B cells that are not positively selected undergo apoptosis. Positively selected B cells can exit the GC as memory B cells and antibody-secreting plasma cells. However, those that remain in the GC are recycled for further rounds of mutation and selection (3, 4), resulting in antibodies of increasing affinity over time (5).

Circulating antibodies and memory B cells generated upon primary infection mediate the secondary humoral immune response upon reinfection with the same or similar antigens. Memory B cells are rapidly reactivated upon reinfection, and ensuing processes increase their frequency and affinity and lead to differentiation into antibody-secreting plasma cells (6, 7). This pathogen-specific humoral memory response can protect against productive reinfection. It is also the basis for vaccination and the reason why booster shots confer more robust protection against infection.

Upon reinfection or reexposure to a vaccine, memory B cells can reenter GCs and undergo affinity maturation (8–10). Memory B cells also expand outside the GC and differentiate into plasma cells (8–10). It is known that B cells can interact with

Author contributions: M.V.B. and A.K.C. designed research; M.V.B. performed research; M.V.B., M.C.N., and A.K.C. analyzed data; M.V.B. and A.K.C. wrote the paper; and M.C.N. contributed and described experimental data and edited the paper.

Reviewers: J.C., HHMI, University of California San Francisco; and T.M., École Normale Supérieure.

Competing interest statement: For completeness, it is noted that A.K.C. is a consultant (titled "Academic Partner") for Flagship Pioneering and also serves as a consultant and member of the Strategic Oversight Boards of its affiliated companies, Apriori and FL72. M.C.N. is on the Scientific Advisory Boards of Celldex, Walking Fish, and Frontier Bio.

[1]To whom correspondence may be addressed. Email: arupc@mit.edu.

This article contains supporting information online at http://www.pnas.org/lookup/suppl/doi:10.1073/pnas.2205598119/-/DCSupplemental.

Published August 25, 2022.

and acquire antigen at the follicle–subcapsular sinus boundary (11–15), and memory B cells might be expanded in such compartments with activated B cells. Recently, it was discovered that memory B cell expansion also occurs in lymph node structures called subcapsular proliferative foci (SPFs) (16). In these structures, memory B cells can bind to and internalize antigen, receive T cell help, and expand rapidly with little or no mutation. In the SPFs, memory B cells also differentiate into plasma B cells and a population of B cells with an RNA expression profile similar to memory B cells (6, 16). Herein, we will refer to affinity-dependent expansion of memory B cells outside the GC as extragerminal center compartment (EGC) processes, which may occur in various compartments such as the SPF.

Despite significant advances over the years, many aspects of the humoral memory immune response are not well understood. (1) What are the determinants of the duration of humoral memory? (2) To what extent do memory B cells enter GCs and undergo further evolution upon reinfection or a booster vaccine dose (8, 9)? (3) How do secondary GCs and expansion of memory B cells outside GCs work together to shape the recall response to the same antigen or its variants? The answers to these questions are fundamentally important and can guide the design of vaccination strategies against evolving viruses such as influenza and emerging severe acute respiratory syndrome coronavirus 2 (SARS-CoV-2) variants of concern. This article focuses primarily on the third question but also provides information pertinent to the second question.

We first developed a computational model to address these questions. Our results suggest that, upon reexposure to the same antigen, existing high-affinity memory B cells are selectively and rapidly expanded in the EGCs. Over longer times, memory B cells that enter GCs can produce even more potent memory B cells and antibodies. GC processes also result in a diverse set of memory B cells, some with low antigen affinities (17). We find that this diversity serves an important purpose upon exposure to a variant antigen. Cross-reactive B cells drawn from this diverse pool of cells may have the highest affinity for a variant antigen. These cells are rapidly expanded in the EGCs to confer protection against infection by a variant antigen. Over a longer time, both memory and naive B cells that enter secondary GCs create a tailored high-affinity antibody response specific to the variant antigen. As the difference between the variant antigen and those encountered previously increases, it becomes more important for naive B cells to seed recall GCs to respond to the variant. We positively tested these computational results in a limited way by analyzing data on memory B cells and antibodies generated after the first and second doses of COVID-19 messenger RNA (mRNA) vaccines. Finally, we studied why expansion of memory B cells outside the GC and secondary GCs may have evolved together to optimally protect organisms from pathogens such as evolving virus families.

Materials and Methods

Our computational model includes processes that occur both in GCs and in EGCs. Upon the first exposure to an antigen, naive B cells seed GCs, undergo affinity maturation, and generate a pool of memory B cells. Upon reexposure to the same or variant antigens, naive and memory B cells can seed secondary GCs and undergo affinity maturation. Memory B cells can also expand in EGCs. These processes included in our computational model are illustrated in Fig. 1.

Model for GC Processes.

Initializing the simulation. Our model for GC processes is based on our past work (18, 19). Naive B cells are drawn from a precursor distribution of B cells that can bind to different epitopes of the antigen and an initial binding free energy distribution drawn from a uniform distribution (detailed further in *SI Appendix*, Supplement 1). The choice of precursor frequencies and method to determine binding free energies are described later. The B cells chosen in this initial step are then tested for their ability to internalize antigen. We have adapted a method from our past work (18) (*SI Appendix*, Supplement 7) to model antigen capture. Briefly, in this model, BCRs bound to antigen are subjected to a pulling force, and depending upon whether the BCR–antigen bond or the antigen–FDC bond breaks, antigen is internalized or not. Our model requires that B cells internalize a small threshold amount of antigen (100 molecules) to seed a GC. B cells that surpass this threshold are randomly selected, with an expected value of 200 clones seeding the GC and undergoing affinity maturation (*SI Appendix*, Supplement 7).

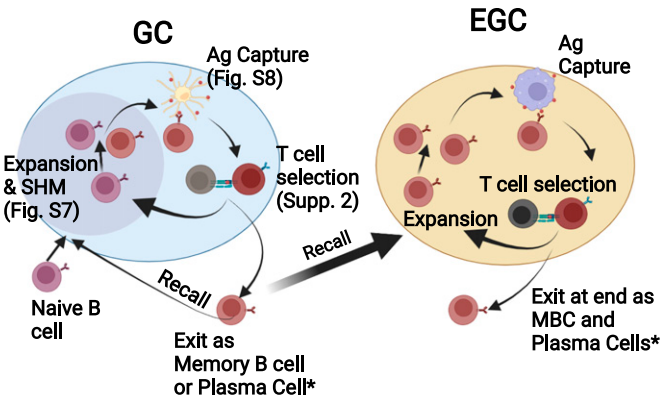

Fig. 1. Agent-based model described in the *Materials and Methods*. Naive B cells enter prime germinal centers, where they expand and mutate, capture antigen, and are selected by T cells. Most are recycled for further rounds of affinity maturation, while others exit as memory B cells. *The model lumps memory B cells (MBCs) and plasma cells into one population. It is assumed that plasma cells are derived from the high-affinity tails of the GC B cell distribution. During the recall response, these MBCs then seed secondary GCs (along with naive B cells) or EGCs. MBCs expanding in the EGC undergo repeated rounds of antigen capture, T cell selection, and expansion. Created with BioRender.com. SHM, somatic hypermutation.

Mutation and selection. In the GC, B cells multiply at a basal rate of 1.5/d. Half of the progeny of the proliferating B cells can mutate. The antigen binding free energy upon mutation is more likely to decrease (lower affinity) because the number of BCR sequences that bind better to a given antigen are fewer than those that bind more weakly. This effect is reflected in experimental data on the effect of mutations on affinity of protein–protein interfaces (20). We use a distribution of affinity changes wherein deleterious mutations are more likely than beneficial ones (*SI Appendix*, Supplement 7). Using other distributions (21) that also reflect this effect does not change qualitative results (*SI Appendix*, Supplement 6).

For the first step of selection, we determine the amount of antigen internalized by a B cell, as described earlier (18) and in *SI Appendix*, Supplement 7. The probability of capture success increases with antigen binding free energy and the amount of available antigen. The amount of available antigen decreases as antigen is captured. The effects of T helper cell selection is incorporated in a coarse-grained way by accounting for the following three observations: A B cell that internalizes more antigen is more likely to display more antigen and succeed in receiving T cell help; B cells that internalize more antigen divide a greater number of times (22); and the availability of a larger amount of T cell help makes selection less stringent, thus reducing the ability to discriminate between B cells that internalize different amounts of antigen (4). These effects are encapsulated in the following formula for the birth rate, β_i, of the ith B cell in the next round of replication and mutation:

$$\beta_i = \beta_0 \frac{C + A_i}{C + \langle A \rangle} \quad [1]$$

where β_0 is the basal birth rate (1.5/d), C increases with the amount of available T helper cells, A_i is the amount of antigen captured by B cell, i, and $\langle A \rangle$ is the mean amount of antigen internalized by all GC B cells that have captured antigen in the current round of affinity maturation. For most of the results

shown, $C = 0$, but we have varied this parameter as noted in context. The qualitative behavior of the model does not change much when C is changed (*SI Appendix*, Supplement 2).

After each round of mutation and selection, most positively selected B cells are recycled for repeated rounds of mutation and selection (3, 4). In our model, 90% of positively selected B cells are recycled, while the others exit the GC as plasma and memory cells. For the purposes of addressing the questions of interest in this article we do not need to distinguish between memory and plasma cells, and so we do not do so.

Model for the binding free energy. Simulating the model described above requires that we be able to compute the binding free energy of a BCR for the antigen. The binding free energy has two components. As described in *SI Appendix*, Supplement 7, one component reflects the "bare" binding free energy without accounting for any steric or geometric effects. Because epitopes on real antigens, like virus spikes, are presented in different geometries, the second component of the binding free energy accounts for such effects. Many virus spikes have a shape that has a globular head and a stalk; examples include influenza and SARS-CoV-2. Our model for antigen geometry is inspired by a coarse-grained representation of the influenza virus's spike, but we incorporate features common to many viruses, and so our qualitative results should be general. In past work (18), the solvent-accessible surface of an influenza spike was coarse-grained into 117-head and 67-stalk epitopes, with the latter being sterically less accessible to antibodies. We have used this geometry as a coarse-grained representation of an antigen. As mutations occur, the bare binding free energy evolves as described above. To account for the differences in geometry and steric accessibility of the different epitopes, we adjusted the bare binding free energy of a BCR for a particular epitope by a fixed factor that is different depending upon the geometry of the epitope (18). This factor is determined by carrying out molecular dynamics simulations. In these simulations, it was assumed that all epitopes have the same bare binding free energy, and then the first passage time was calculated for an antibody binding to each epitope. Thus, for each epitope, we computed an on-rate for the binding of one arm of the BCR/antibody to the antigen and a second conditional on-rate for the binding of the second arm of the antibody. These on-rates correspond to epitope-specific steric corrections to the bare binding free energy (*SI Appendix*, Supplement 7).

Of the 184 epitopes in our model, a small number (13) are the same for all variant antigens. The others can be different, as described below. There are 40 naive precursors per epitope for the 13 epitopes that are shared by all variants (520 naive B cells) and 8 naive precursors per epitope for the others (1,368 naive B cells), resulting in about 27.5% of naive B cells binding to conserved epitopes. Of these 1,888 naive B cells, roughly 200 will seed the GC (*SI Appendix*, Supplement 7). Our qualitative results do not depend on our arbitrarily chosen precursor frequencies (*SI Appendix*, Fig. S10). Similarly, changing the number of conserved epitopes does not change the qualitative results, as it is identical to changing the number of precursors.

Model for variant antigens. We study the recall response to the same antigen that was encountered previously, as well as variant antigens. We model how different the variant is from that to which there was past exposure by defining a correlation factor. If the correlation factor equals -1, the variant is as different as it can be within our model; a value of $+1$ indicates that the new antigen is identical to the previously encountered antigen. A BCR will have different binding free energies, E_1 and E_2, to an epitope on antigens 1 and 2, respectively. When the GC simulation is initialized, the bare binding free energy for an epitope on the variant antigen, E_2, is drawn from a copula (23) in a way that depends upon E_1. The correlation factor between many samples of E_1 and E_2 equals the prescribed value. As examples, when the correlation factor is 1, the binding free energies are the same, and when the correlation is -1, the binding free energies are equal and opposite.

The change in bare binding free energy upon mutation for an antigen and its variant is also related by the correlation factor. Two numbers, x_1 and x_2, are drawn from a copula with a uniform distribution between 0 and 1. When the correlation factor is -1, $x_2 = 1 - x_1$. To obtain the changes in binding free energy, ΔE_1 and ΔE_2, x_1 and x_2 are used as the percentile of the change in binding free energy as obtained from the cumulative distribution function of the changes in binding free energy upon mutation. For example, if x_1 is 0.2, then ΔE_1 will come from the 20th percentile of the distribution of changes in binding free energy. This corresponds to $\Delta E_1 = -0.701$. If the correlation factor is -1, then x_2 will be 0.8, representing the 80th percentile. This means $\Delta E_2 = 0.044$. This example is illustrated in *SI Appendix*, Fig. S7*B*.

Model for EGC Processes. In our model, memory B cells are allowed to expand in EGCs in an antigen-dependent process (16). The dynamics are the same as in the model for the GC, except for the following points: (1) Because there is little or no activation-induced cytidine deaminase expression in SPF B cells (16), we assume that there is no mutation (allowing a small amount of mutations does not change qualitative results; *SI Appendix*, Supplement 8); and (2) the number of generations of replication and selection that occur outside the GC is not known, and so we have studied the effects of varying this parameter (*SI Appendix*, Supplement 5). The strictness of T cell help may also be different in the GCs and EGCs, but such differences have not been explored.

For computationally tractability, only about 22% of memory B cells generated after the first exposure to an antigen were "sampled" and eligible to seed a secondary GC or EGC. This was modeled by allowing memory B cells to decay by about 78% (exponential decay of 1.5 half-lives). This "decay" is more than the two- to threefold decay of memory B cells over the first ∼100 d observed in experiments (24, 25). The difference in the decay rates compared to experiments does not affect qualitative results for two reasons. First, choosing a different decay rate leads to a difference in the ratio of memory B cells to naive B cells in the secondary GC. This parameter can instead be directly controlled in our simulations, and we studied the effects of such variations (Figs. 2 and 3). Second, fewer initial memory B cells in the EGC results in a higher number of generations of replication because it takes longer to consume antigen. We directly studied the effects of varying the number of generations (*SI Appendix*, Supplement 5).

Antibody Sequences from SARS-CoV-2 Vaccinated Humans. Antibodies were obtained from a longitudinal cohort of SARS-CoV-2 mRNA vaccinated individuals (26). All participants provided written informed consent before participation in the study, and the study was conducted in accordance with good clinical practice principles. The study was performed in compliance with all relevant ethical regulations, and the protocol (DRO-1006) for studies with human participants was approved by the institutional review board of The Rockefeller University. B cells expressing antibodies that bind to the receptor binding domain of SARS-CoV-2 were purified by flow cytometry and their antibody genes cloned by established molecular biology methods. Binding and sequence characteristics for individual antibodies were as described (26).

Results

Relative Roles of GC and EGC during the Recall Response to the Same Antigen. We first used our computational model to consider the recall response upon reexposure to exactly the same antigen. This could happen due to natural infection, or the reexposure could be due to a booster shot of a vaccine. The distribution of binding free energies for the memory B cells that were generated in the GC upon the first infection or the first dose of a vaccine (prime) is shown as identical light blue curves in Fig. 2 *A* and *B*. The EGC and GC processes act on this B cell population if memory B cells alone enter secondary GCs. The binding free energy distributions emerging from the EGC (red curve) and recall GCs (dark blue curve) are also shown. In the EGC, there is selective expansion of the available higher-affinity memory B cells. This is why the median affinity of the B cells generated in the EGC is higher than that of the memory B cells generated after the prime (compare light blue and red curves in Fig. 2*A*). For the same reason, the frequency of high-affinity B cells and antibodies represented by the high-affinity tail of the red curve is also higher than that of the existing memory B cells. The affinity distribution of the products of the EGC is dependent on the number of generations of replication, with more generations resulting in a larger increase in median affinity and the population in the high-affinity tail of the distribution (*SI Appendix*, Supplement 5).

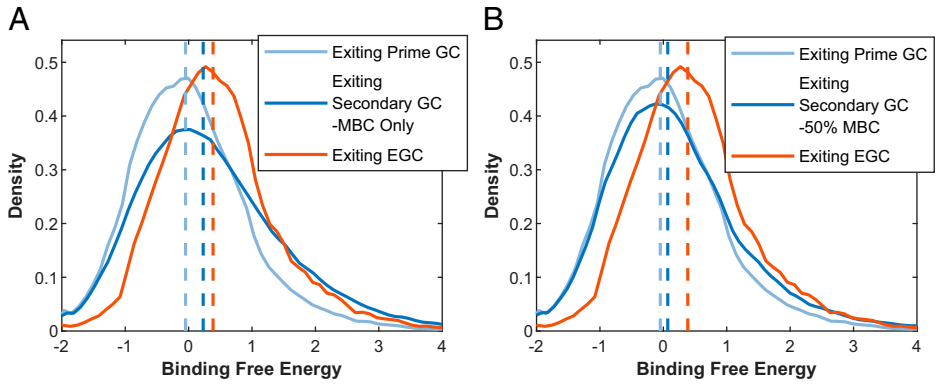

Fig. 2. Probability distributions of the binding free energies of different populations of B cells obtained using our computational model are shown. The vertical dashed lines represent median affinities. The light blue curves show the memory B cells (MBCs) available after the first antigen exposure, the red curves show EGC products after reexposure to the antigen, and the dark blue curves show secondary GC products. (*A*) Only MBCs seed secondary GCs. (*B*) Equal proportions (50/50 mixture) of naive and MBCs seed secondary GCs.

Memory B cells (generated during the prime) that seed secondary GCs are subjected to mutation and selection, resulting in a broader binding free energy distribution than the EGC products (compare red and dark blue curves in Fig. 2*A*). Because mutations are more likely to be deleterious rather than beneficial (20), the median binding free energy of the EGC products is higher than that of the GC products. However, the GC products have a fatter high-affinity tail and generate the highest-affinity antibodies. This is because beneficial mutations can be positively selected in the GC to generate the best antibodies, whereas the EGC can only expand the existing memory B cell distribution.

Secondary GCs can also be seeded by naive B cells (8). The relative numbers of memory and naive B cells seeding these GCs are probably determined by the precursor frequencies of naive B cells specific to the antigen and the affinities of the memory B cells generated during priming. Fig. 2*B* shows our simulation results when the secondary GC is seeded by an equal number of naive and memory B cells. Now, the naive and memory B cells compete during the recall response, and so the median affinity of GC products is lower than when only memory B cells seed secondary GCs. This difference is made evident by comparing the differences between the medians of the dark blue and red curves in Fig. 2 *A* and *B* because the red curves remain the same as only memory B cells are expanded in the EGC. The GC processes still generate the best antibodies (see right tails of distributions shown in Fig. 2*B*), but this effect is diminished when naive B cells also seed GCs. If only naive B cells seed the secondary GCs, the model's resulting affinity distribution would be statistically identical to that generated upon priming.

Our results thus far regarding the recall response can be summarized as follows. The processes that occur in the EGC selectively expand the higher-affinity existing memory B cells. The products of secondary GCs exhibit a wider affinity distribution compared to those emerging from the EGC because mutations can be both beneficial and deleterious. The median affinity of GC products is lower than that of EGC products because many mutations can be deleterious. However, the secondary GCs produce the highest-affinity antibodies. As processes in the EGC occur faster, its products provide the first protective recall response generated from the higher-affinity memory B cells available after the prime. The secondary GCs produce better antibodies over longer times. If naive B cells also enter secondary GCs, this advantage is diminished. These results raise the question of whether the low-affinity products of secondary GCs are simply an unavoidable byproduct of mutation and selection processes or whether they may serve a useful purpose.

Relative Roles of GC and EGC during the Recall Response to a Variant Antigen. Next we used our computational model to consider the recall response to an antigen that is a variant of the one that led to the first exposure. For any two variant antigens, some epitopes will be the same (conserved) for both antigens. As described in *Materials and Methods*, the variable epitopes can differ to differing extents, which is quantified in

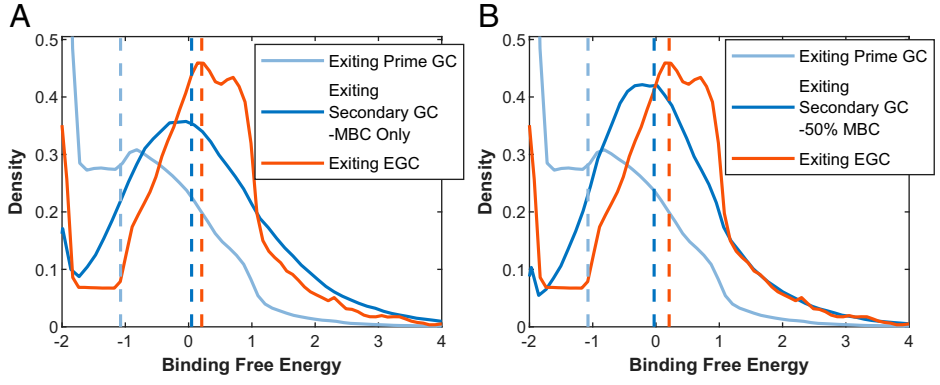

Fig. 3. Probability distributions of the binding free energies of different populations of B cells to a variant antigen obtained using our computational model are shown. The vertical dashed lines represent median affinities. The light blue curves show the affinities of memory B cells (MBCs) generated during the first exposure, the red curves show the affinities of EGC products after reexposure to the variant antigen, and the dark blue curves show affinities of secondary GC products. (*A*) Only MBCs seed secondary GCs. (*B*) Equal proportions (50/50 mixture) of naive and memory B cells seed secondary GCs.

our model by the correlation factor describing the binding affinities of the same BCR to two variant epitopes. The results shown in Fig. 3 are for a variant antigen that is as different as our model allows (correlation of −1; see *Materials and Methods*), but the qualitative results are the same for other variant antigens (*SI Appendix*, Fig. S4).

The light blue curve in Fig. 3*A* shows the affinity distribution of the available pool of memory B cells generated by the prime. It is very different from the light blue curves in Fig. 2 (with many more low-affinity B cells) because the antigen is a variant of the priming antigen. The red curve in Fig. 3*A* shows that, in the EGC, the highest-affinity memory cells are selectively expanded, resulting in a higher median affinity compared to the existing memory pool. Note that these cross-reactive B cells expanded in the EGC are unlikely to have high affinity for the priming antigen. They consist of the few clones that target the conserved epitopes and others that also bind with high affinity to the variant epitopes. These memory B cells exist because of the diversity created in GCs, which enables an early recall response that helps control variant pathogens, consistent with experiments using heterologous flavivirus (27, 28). We will emphasize this point again in a later section.

The cross-reactive B cells also enter secondary GCs. As the dark blue curve in Fig. 3*A* shows, over longer times, secondary GCs result in the highest-affinity antibodies to the variant antigen. This is because the high-affinity cross-reactive memory B cells can evolve by mutation and selection to improve their affinity for the variant antigen. Because deleterious mutations evolve in the secondary GCs, the affinity distribution of these GC products is wider than that of EGC products, and the median is also lower. The diversity created by the secondary GCs would be helpful for producing a rapid protective response in the EGC to yet another variant antigen in the future.

We next studied how the results described in Fig. 3*A* change if naive B cells also seed secondary GCs. Fig. 3*B* shows the results when secondary GCs are seeded with equal proportions of naive and memory B cells. As in Fig. 2*A*, the median affinity of GC products is lower than that of the EGC products, but now even the highest-affinity products of the secondary GCs and the EGC are comparable. When a significant proportion of naive B cells enter secondary GCs, the principal purpose of the secondary GCs appears to be to create diversity rather than produce high-affinity antibodies. In *SI Appendix*, Fig. S11 we show some conditions where the median affinity increases with the proportion of naive B cells seeding secondary GCs. These circumstances include cases where the priming antigen and the variant share no conserved epitopes, or T helper cell selection does not differentiate well between B cells of different affinity.

Data from Humans Vaccinated against COVID-19 Are Consistent with the Computational Results. The computational results described above apply to recall responses upon natural infection or vaccination. Analyses of sera obtained from individuals vaccinated with two doses of an mRNA-based COVID-19 vaccine provide a dataset to further explore the relative roles of the EGC and GCs during recall responses and examine whether the data are in harmony with the computational results. Cho and colleagues sampled B cells from 11 individuals after the first and second doses of the Moderna or Pfizer-BioNTech vaccines (26). The samples were collected an average of 2.5 wk after the first dose and an average of 1.3 and 5 mo after the second. A total of 2,324 B cells were sequenced and grouped into clonal families. We constructed phylogenetic trees by using MATLAB's seqlinkage function to minimize pairwise distance between IGH nucleotides for each clonal family. If a phylogenetic tree contained two or more identical sequences, with at least one sequence sampled after the second dose, then it was assumed that these clones were expanded in the EGCs (*SI Appendix*, Supplement 14). This approximation is very conservative, as a low rate of mutation is possible in the EGCs. For this reason and because the sequences are significantly undersampled, we can identify only a small subset of cells that were expanded in EGCs during the recall response to the second dose. The affinities of the 458 antibodies from the sampled B cells were measured against the SARS-CoV-2 receptor binding domain. These data, quantified as measured half maximal effective concentration values, were converted to a metric similar to the binding free energy by taking the negative log of half maximal effective concentration and using a reference affinity (the lowest-affinity 1.3-mo clonal antibody). Out of an abundance of caution in avoiding sampling bias, only B cells that had affinities measured at the specified timepoint (prime or 1.3 mo) were included. For example, if an EGC B cell's affinity was measured before the boost, and it had a clone of identical sequence after the boost whose affinity was not measured, we did not include this affinity in the data after the prime. Graphs that include such sequences, which are inferred to have the same affinity because they have identical sequences, are shown in *SI Appendix*, Supplement 15, and the results are qualitatively the same.

Three B cells sampled after the first dose of the vaccine for which affinity measurements were available were identified by us as those that were later expanded in the EGC after the second dose. Affinity measurements were available for B cells belonging to other clonal families sampled after the first dose and for B cells not belonging to these clonal families (singlets). Fig. 4*A* shows the affinities of the clones sampled after the first vaccine dose that were later selected in recall EGCs and the other B cells sampled after the first dose. The clones identified as those that were later expanded in the EGC have a higher mean affinity and a lower variance compared to the other B cells. These data are consistent with the notion that high-affinity memory B cells available after the first exposure to the antigen are selectively expanded in the EGCs upon reexposure. This point is reinforced by our analyses of the cells sampled after the second vaccine dose.

From the cells sampled after the second vaccine dose, measured affinities were available for 19 of the ones we identified as being expanded in the EGC. Fig. 4*B* shows that these cells' affinities are also narrowly distributed around a high value. The other clones sampled after the second dose are probably derived from secondary GCs and exhibit a higher diversity of affinities. Importantly, this population of B cells also contains the highest-affinity clones (compare blue and red curves in Fig. 4). These data are consistent with our computational results, which show that the EGC selectively expands the high-affinity memory B cells, and the products of the GC have a wider variance and contain the highest-affinity B cells and antibodies (compare dark blue and red curves in Fig. 2). We note that our analyses of the human data after vaccination are limited by the paucity of sequences for which affinities were measured. However, the available data support the computational results reported in Fig. 2.

We also examined the sequences obtained 5 mo after the second dose of COVID vaccines. These data do not directly speak to the issue of the recall response. However, we found that a large fraction of the EGC clones we identified after 5 mo were also observed after 1.3 mo and exhibit characteristics similar to that shown in Fig. 4 (*SI Appendix*, Fig. S16).

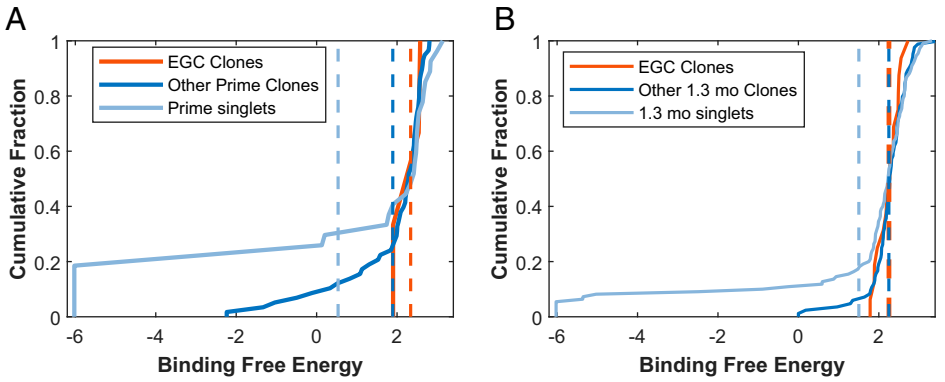

Fig. 4. Clinical data obtained from humans who received COVID-19 vaccines. (*A*) The cumulative distributions of binding free energies of B cells sampled after the first dose of the vaccine (prime). Data for those identified to be expanded subsequently in EGCs (red), part of other clonal families (blue), or singlets (light blue). Dashed lines indicate means. (*B*) Similar data as in panel *A* for cells sampled after the second vaccine dose (boost).

An Evolutionary Perspective on the Relative Roles of EGCs and GCs during the Recall Response. In the spirit of past studies exploring the evolutionary origins of the immune system (29, 30), we next explored whether evolution selected for the relative roles of the EGC and GC processes described above because organisms experienced repeated exposure to the same pathogen and variants of the same family of pathogens. We developed a simple model of infection and reinfection whose parameters could be varied to study the consequences of variations in the relative roles of the EGC and GC.

The first ingredient in this model is a description of the essence of GC processes, but it neglects stochastic effects. The resulting mean-field dynamical equation is (Fig. 5 *B* and *C*):

$$dB_{i,\mathrm{GC}}/dt = r_{\mathrm{GC}} B_{i,\mathrm{GC}}(f_i/\langle f\rangle) * (1-\mu) + [\mu/(N-1)]\; r_{\mathrm{GC}} \sum_{j\neq i}\left(f_j B_{j,\mathrm{GC}}\right)/(\langle f\rangle) - \mathrm{PC}_{\mathrm{GC}} B_{i,\mathrm{GC}} \quad [2]$$

$B_{i,\mathrm{GC}}$, the number of B cells of type i in the GC, and each type of B cell are characterized by a fitness, f_i, that quantifies the ability to be positively selected and replicate. A three-dimensional shape space model (31) is used to calculate the fitness of a B cell, i. The antigens and B cells are represented as points in this three-dimensional space. Past work has shown that a higher dimensionality does not change qualitative results (32, 33). For the first infection, the antigen is located at the origin, and the initial pool of B cells is distributed uniformly in the space spanned by the coordinates $[(-1,-1,-1),(1,1,1)]$. The shape space is discretized in units of 0.2 units in each dimension. The fitness is calculated as $(1–\mathrm{d}_{\mathrm{B-A}}/\sqrt{3})$, where $d_{B\text{-}A}$ is the Euclidean distance between the B cell and the antigen in shape space (Fig. 5*A*). B cells evolve by mutation, with a rate equal to μ. The value of μ was set equal to 0.05. The results are qualitatively the same unless the mutation rate becomes very high ($\mu > 0.35$) when the response to a variant pathogen changes (*SI Appendix*, Fig. S12). The first term in Eq. **2** describes the replication of B cells of type i minus the mutations to other types of B cells. The second term describes mutations in other types of B cells that result in transitions to B cells of type i. N is the total number of B cell types; N equals 1,331 (11^3) because we discretize shape space by using 11 bins between –1 and 1 in all three dimensions (distance between bins is 0.2). The inverse of r_{GC} sets the time scale characterizing GC processes. The third term represents GC B cells terminally differentiating into plasma cells. $\mathrm{PC}_{\mathrm{GC}}$ is the rate at which GC B cells differentiate into plasma cells and create antibodies. This term is small (6) compared to the others in Eq. **2** and was ignored when we simulated Eq. **2**.

For the first exposure to an antigen at the origin of shape space, Eq. **2** is simulated for a time, t, equal to 32 * τ, where τ

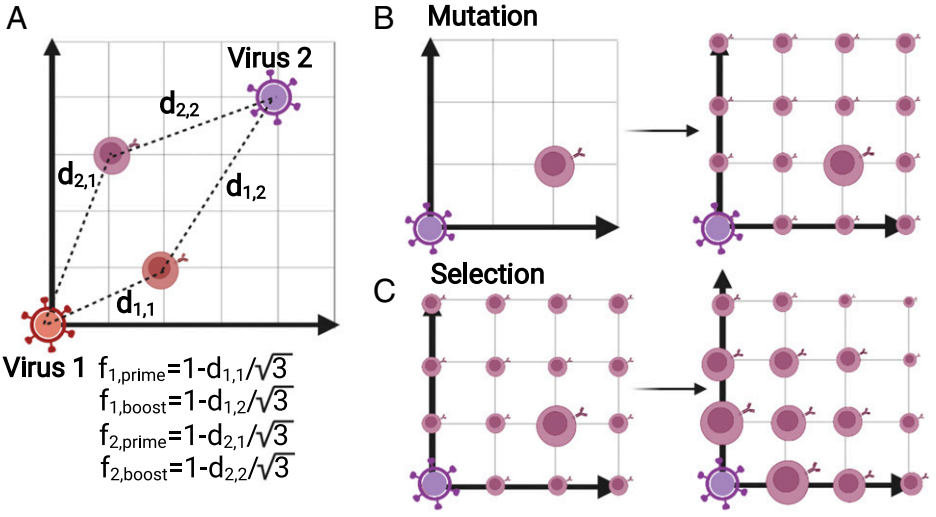

Fig. 5. Illustrations of B cells in shape space. (*A*) Example calculation of fitnesses, *f*, for B cells binding to viruses 1 and 2. (*B*) One B cell clone undergoing mutation across shape space. The size of each B cell represents the clonal size. (*C*) Expansion of B cells is dependent upon relative fitness. The size of each B cell represents the clonal size. Created with BioRender.com.

is the inverse of the rate of replication of the antigen r_{antigen} (see below). The initial condition is 3,000 total B cells. The resulting distribution of B cells becomes the memory pool that is available upon reexposure to the same or variant antigen. In some simulations, for reasons described in context, the memory pool is arbitrarily taken from the distribution at an earlier timepoint of $t = 6 * \tau$ (34). If the second antigen to which one is exposed is the same, it is still located at the origin. We also show results by using a variant antigen placed at the location [0.8, 0.8, 0.8] in shape space. This represents a large antigenic distance of 80% of any individual BCR's radius of binding ($d_{B-A} < \sqrt{3}$).

When we challenge the available pool of memory B cells with the same or variant antigen, the recall response involves both GC and EGC processes. The fitness of each B cell for the antigen is calculated in the same way as before, and the GC processes that ensue are still described by Eq. **2**. The dynamics of the EGC is described by the following mean-field equation for each type of B cell that enters the EGC (Fig. 5*C*):

$$dB_{i,\text{EGC}}/dt = r_{\text{EGC}} B_{i,\text{EGC}} f_i/\langle f\rangle - \text{PC}_{\text{EGC}} B_{i,\text{EGC}} \quad [3]$$

The inverse of r_{EGC} defines the time scale of EGC processes, which is known to be faster than that corresponding to r_{GC}. The second term represents EGC B cells terminally differentiating into plasma cells. For the results shown in the main text, this term is ignored in Eq. **3** because the average population growth of EGC B cells depends only upon the difference ($r_{\text{EGC}} - \text{PC}_{\text{EGC}}$). The average population growth of EGC B cells is what is observed experimentally (6). We find that ignoring the differentiation of plasma cells in Eq. **3** does not meaningfully change the results (*SI Appendix*, Fig. S13).

For the boost GC and boost EGC each, there are 3,000 total B cells distributed across shape space according to the memory pool's affinity distribution. Upon a recall infection, B cells that had a low fitness to the prime antigen may be a small, fractional amount. If a given $B_i(t = 0) < 1$, then $B_i(t = 0) = 0$. Note that the recall GC will be able to quickly populate these empty $B_{i,\text{GC}}$ locations via mutation, while the EGCs cannot, so the EGCs will only expand the existing clones. As the number of B cells becomes large, the model behaves like a continuous model without the cutoff for $B_i(t = 0) < 1$ noted above (*SI Appendix*, Supplement 13).

The B cells in the GC and the EGC can produce antibodies because these cells can differentiate into plasma cells. The dynamics of the population of antibodies of type i, A_i, is modeled by production of antibodies from plasma cells and consumption of antibodies bound to virus by diverse mechanisms involving innate immunity. The equation describing these effects is:

$$dA_i/dt = \text{PC}_{\text{EGC}} B_{i,\text{EGC}} + \text{PC}_{\text{GC}} B_{i,\text{GC}} - k_{ab} * f_i * A_i * V \quad [4]$$

The first two terms in Eq. **4** represent the production of antibodies in the EGC and the GC. PC_{EGC} and PC_{GC} represent the rates of production of antibodies secreted by B cells in the EGC and the GC, respectively. These rates encapsulate the rates at which B cells differentiate into plasma cells and produce antibodies. PC_{EGC} is considered to be larger than PC_{GC}, because a considerably larger fraction of SPF/EGC B cells become plasma cells compared to GC B cells (6). The third term represents consumption of antibodies. Antibodies bind and clear the antigen at a rate proportional to their fitness and a basal scale, k_{ab}, for the rate of this clearance process. The quantity, V, in Eq. **4** represents the number of antigen particles.

For the first infection, a small number of antigen particles (10) represent the initial antigen load. Upon reinfection, the memory B cell population is challenged with an initial antigen load equal to 1,000 antigen particles. This higher viral load is required to generate a meaningful infection because the primed immune system rapidly clears infection with a low initial viral load, and it is difficult to study the dynamics. Changing the boost viral load to 100 or 3,000 does not change the qualitative results. The amount of antigen (V) changes with time according to the following mean-field equation:

$$dV/dt = r_{\text{antigen}} * V - \textstyle\sum_i (f_i * A_i) * k_{ab} V \quad [5]$$

The first term above represents the growth of the antigen at a rate r_{antigen}. The second term is the rate at which the antigen is cleared by antibodies.

Eqs. **2** and **4** are simulated until $t = 32 * \tau$ or the antigen load is larger than 10^9, a large number meant to represent severe consequences for the patient. When the antigen load is less than 1, the virus has been cleared.

First, we consider reinfection with the same antigen. We vary the relative roles of the EGC and GC by varying the relative rates of the processes that occur therein. Specifically, we vary the quantities, $\alpha = r_{\text{EGC}}/r_{\text{antigen}}$. and $\beta = r_{\text{GC}}/r_{\text{antigen}}$. The case where α equals zero describes a situation where only the secondary GCs can protect against reinfection. We calculated the maximum viral load during reinfection as α and β were varied (Fig. 5*A*). A large change in r_{GC} (going from left to right) has a small effect on the maximal viral load compared to slightly changing α or r_{EGC} (traversing from curve to curve). These results show that during a recall response the EGC plays the dominant role in combating infection. This is because EGC B cells differentiate into a higher fraction of plasma cells, as shown in the SPF (6) (PC_{EGC} is greater than PC_{GC}), because they have a higher growth rate (6) (α is greater than β) and because the mean fitness is higher for the products of the EGC (Figs. 2–4). The findings in Fig. 6*A* are consistent with experimental data showing serum responses to flaviviruses are similar with or without secondary GCs (28). The results in Fig. 5*A* are robust to changes in parameters. A higher k_{ab} represents faster viral clearance by antibodies and reduces the required α or β needed for protection. A higher initial antigen load requires a higher value of α or β to combat the virus.

The results shown in Fig. 6*A* suggest that EGCs evolved to react quickly by selectively expanding the high-affinity memory B cells with little or no mutation and quickly ramping up antibody production upon reinfection with the same antigen. GC processes occur over longer times, and waiting for this duration would not allow the recall response to quickly suppress infection and prevent disease. So why did evolutionary forces not lead to abrogating secondary GCs, which consume metabolic resources? Over longer times, the GC does produce better antibodies, but the results we discuss next suggest an even stronger reason why secondary GCs are very important.

Fig. 6*B* compares the results of our simulations upon reinfection with the same antigen and a variant as $r_{\text{GC}}/r_{\text{EGC}}$ (or β) is varied. As the solid lines show, infection with a variant leads to higher antigen loads (solid red and green lines in Fig. 6*B*). This is because the antibodies produced by the EGC are not as potent. Fig. 6*B* also shows the importance of primary and secondary GCs. Increasing β specializes the prime GC memory B cell pool more to the original antigen. This lack of diversity makes the response to a variant antigen worse. As β increases to much larger values, the number of antibodies produced by secondary GCs increases, allowing better control of the variant antigen. Since r_{GC} is smaller than r_{EGC} (6), β is unlikely to be so high, and so our results suggest that the diversity generated in GCs is very important for protecting against future infections by variant antigens. To highlight the importance of the diversity created by the GC, we also studied a situation when the memory B cell pool available

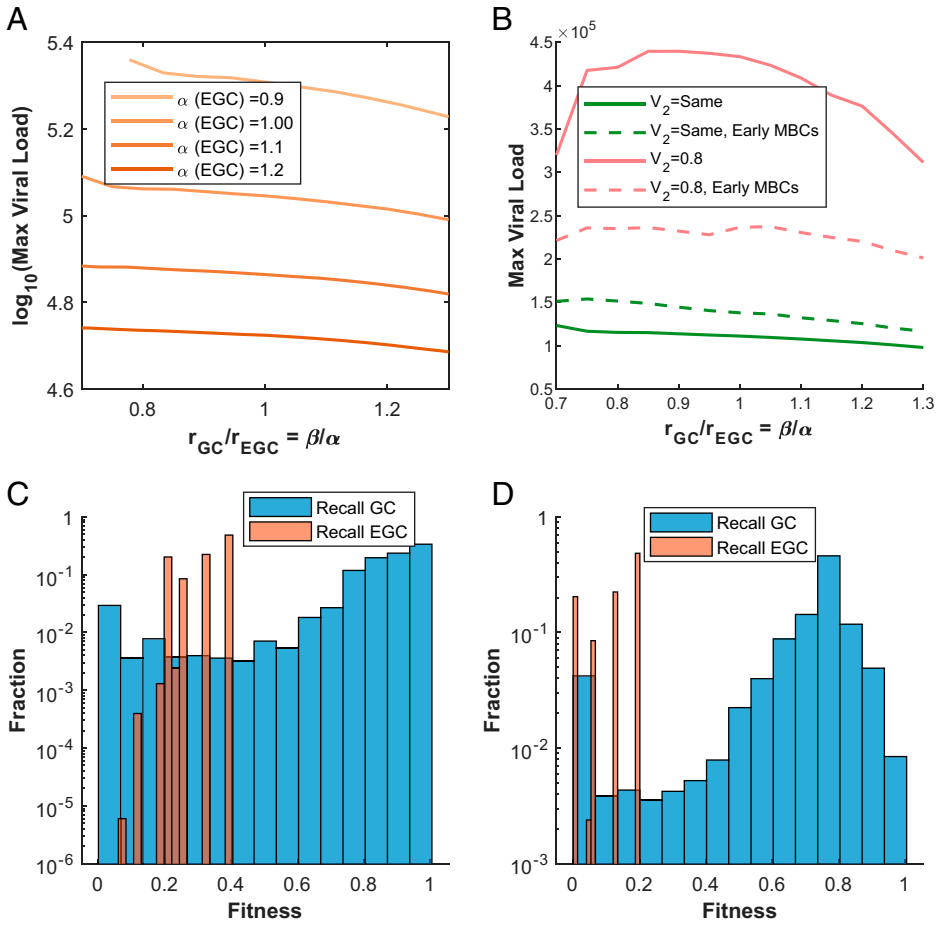

Fig. 6. Results obtained using the evolutionary model. (*A*) The effect of changing the relative values of α (r_{EGC}/r_v) and β (r_{GC}/r_v) on the $\log_{10}$ (maximum viral load) upon reinfection with the same antigen. Different lines show different values of α, the scaled EGC growth rate. (*B*) Comparing the maximum viral load upon reinfection with a variant antigen and the same antigen for different values of r_{GC}/r_{EGC}, with α = 1. The red lines represent a distant variant at the point [0.8, 0.8, 0.8] in shape space (see text), while the green lines represent the same antigen. The dashed lines represent simulations where only earlier B cells ($t = 6 * \tau$) leave the GC as memory B cells. (*C* and *D*) The role of diversity created in the GC. The fitness distributions for GC and EGC products after the recall response ($t = 32\tau$) with a variant antigen at [0.8, 0.8, 0.8] when α = β = 1. (*C*) The fitness distribution to the antigen at [0.8, 0.8, 0.8] or (*D*) The fitness distribution to the antigen at [1, 1, 1] (nearby variant).

after the first infection is restricted to those that existed at an early timepoint in the GC (36) (dashed line) rather than at the end of the GC (solid lines). For reinfection with the same antigen, this results in poorer control of reinfection. However, the EGC and GC antibodies respond better to variant antigens if the memory B cells emerge earlier in the primary GC because these cells are more diverse and less specialized against the first antigen.

Upon reinfection, the secondary GCs can generate bespoke antibodies tailored to the new variant (Fig. 3). Fig. 6*C* shows the distributions of fitnesses to the variant antigen at the end of the recall GC and EGC. The new diversity generated in the recall GC populates the highest-fitness clones that did not previously exist and thus cannot be expanded in the recall EGC. The importance of the recall GC-created diversity for infections with future variants is emphasized in Fig. 6*D*. Here we show the distribution of fitnesses of the memory B cell population for a nearby variant located at [1, 1, 1] after the second infection, with the variant antigen located at [0.8, 0.8, 0.8]. The recall EGC after the second infection can only expand preexisting memory B cells, which are biased toward the first antigen, but the recall GC generates B cells of low affinity to the second variant that have high affinity to the variant at [1, 1, 1]. If the secondary GCs do not create this diversity, a third infection with a nearby variant antigen would not be controlled as effectively by the resulting EGC response. This result is related to ideas described recently based on concepts in decision theory (35, 36). Therein it was suggested that generating diversity during affinity maturation and later recalling such responses may have emerged over evolutionary time scales to optimally protect against viruses that evolve to a modest degree over time.

The results shown in Fig. 6 can be summarized as follows. The more rapid EGC response is important for controlling the pathogen's proliferation while the GC processes are completed, thus decreasing the risk of severe disease. The secondary GCs generate the most potent responses over time, enabling greater protection upon subsequent exposure to the same antigen. Importantly, they also generate a diverse pool of B cells, and upon exposure to yet another variant antigen, the cross-reactive clones are rapidly expanded to provide the best protection possible while the GC process generates a bespoke potent response for the new variant. Thus, the relative roles of EGC and GC processes may have evolved because they are both essential for protection against evolving families of pathogens that complex organisms have been exposed to for a long time.

Discussion

Upon first exposure to a pathogen, the adaptive immune system responds by generating antibodies and activated B cells and T cells specific for the infecting agent. Importantly, after

an infection is cleared, a memory of this past exposure is imprinted in the form of circulating antibodies and memory B cells and T cells. This pathogen-specific immune memory is the basis for vaccination. In this article, we used computational modeling to study the way in which the humoral memory response is recalled upon subsequent exposures to a pathogen or vaccines. Our results suggest that the expansion of memory B cells outside the GC (in structures such as the SPF) and secondary GCs play complementary roles in protecting organisms from reinfection. These processes also enable protection from future infections by variant antigens from the same family of pathogens.

In addition to antibodies, a diverse repertoire of memory B cells is created by GCs during the first exposure to an antigen. Upon reinfection with the same antigen, two processes ensue. In the EGCs, high-affinity memory B cells are quickly selectively expanded, and these differentiate into plasma cells that produce antibodies and memory B cells (6, 16). This generates a narrow distribution of high-affinity antibodies, with a higher median than the original pool of memory B cells (Fig. 2). Thus, a rapid protective response based upon some of the best available memory B cells is generated. Over longer times, secondary GCs can produce even more plasma and memory cells that encode high-affinity antibodies by additional mutation and selection (Fig. 2). Importantly, GCs, including secondary GCs, generate a diversity of cells, some with low affinity (17). Our analyses of limited amounts of sequence and affinity data obtained after the first and second doses of mRNA vaccines for SARS-CoV-2 (26) are consistent with these computational results (Fig. 2). Antibody sequences that are likely to have been generated in the EGC (based on phylogenetic analyses) consist of a narrow distribution of high-affinity clones (Fig. 4). The sequences that probably evolved in secondary GCs exhibit a broader distribution of affinities but include the highest-affinity clones (Fig. 4).

These results led us to investigate the utility of the diversity generated in GCs. Upon reinfection with a variant antigen that differs from the first exposure, the available pool of memory B cells consists mostly of those that have a low affinity for the variant antigen, with only a few high-affinity cells (Fig. 3). The latter cells either target conserved epitopes (which in our model are few) or are the memory B cells with low affinity for the original antigen, but high affinity for the variant, that exist because of the diversity generated in the prime GC. In the EGC, these higher-affinity cross-reactive memory B cells are rapidly and selectively expanded to provide the best early protective response possible (Fig. 3). This response would not be possible without the diversity generated by GCs. Over longer times, the secondary GCs produce the highest-affinity responses tailored to the variant antigen (Fig. 3). However, secondary GCs also generate more diversity, which could help protect against future infection with yet more variants. This generation of GC diversity in addition to EGC expansion of the highest-affinity memory B cells acts as an optimal bet-hedging strategy to deal with variant viruses (35, 36).

We also explored why evolution may have led to complementary roles of the EGC and GCs for the recall response. Our results (Fig. 6) suggest that the recall antibody response due to expansion of memory B cells outside the GC is critical because this process is faster (6), it selectively expands higher-affinity cells that differentiate into plasma cells, and more antibodies are created in the EGCs than the GC (6). This is also true for the recall response to a variant antigen, which results in expansion of the cross-reactive memory B cells that exist because of the diversity created during the prime GC. The latter result is consistent with experimental results that show that secondary GCs contribute weakly to the serum response to infection with heterologous flaviviruses (28). Our results also make clear the critical role of diversity created in secondary GCs for protection against future infections with variants. These findings suggest that the selection force imposed by repeated infection by the same pathogens or their variants probably shaped the complementary roles of EGC and GC processes seen today.

Our results also suggest that exit of memory B cells from the GC at earlier timepoints may help protect against future infection with variants, as the GC population at that time is more diverse (Fig. 6*B* and *SI Appendix*, Supplement 3). This may explain why some experiments suggest that memory B cells exit the GC earlier and may come from lower-affinity memory B cells (17, 37). Of course, over longer times GCs produce the highest-affinity products for any given antigen. This result provides a rationale for why plasma cells are thought to be selected from high-affinity clones (38) and at later timepoints (37) during GC reactions (39).

Our results should be robust to the degree of biological complexity included in the model, as they are based on a few main principles. Indeed, this is the reason that the coarse-grained mean-field evolutionary model is in harmony with the more complex stochastic agent-based model. By including the biological complexities of processes that occur in the GC and EGC, we were able to demonstrate that the results we describe are not because of some gross simplification of the biology in a more coarse-grained model. Using our model, we could also describe the robustness of our findings to variation in parameters that describe biologically realistic processes.

Recent experiments in mice have highlighted that memory B cells may not dominate in seeding recall GCs (8). While the extent to which new naive B cells enter secondary GCs is probably determined by many factors, such as the precursor frequencies and affinities of naive and memory B cells (11, 40, 41), our results suggest an evolutionary benefit. Upon reinfection with a variant antigen, populating the recall GCs with only memory B cells may actually hinder the development of the highest-affinity memory B cells and antibodies in the GC (*SI Appendix*, Fig. S11). This is because the evolutionary paths needed for many memory B cells to acquire high affinity to the variant may be more unlikely than those of new naive precursors with higher initial affinity for the variant. This result has been shown with related influenza viruses in mice, although it may be caused by an inability to further mutate B cell receptors (42). Moreover, naive B cells seeding secondary GCs may help create diversity that is beneficial for protection against future variants.

We hope that our work will motivate further studies of the role of diversity generated in GCs and synergy between EGC and GC responses in conferring protection from reinfection. These issues may be especially important in the context of vaccination. For example, how can simple vaccine formulations be designed to protect against variants that may emerge, such as the SARS-CoV-2 variants that have caused so much havoc. Also, the implications of our study for eliciting broadly neutralizing antibodies that target specific conserved epitopes on spikes of highly mutable viruses, like influenza and HIV, also need to be explored. Future work should include consideration of the effect of the EGC's antibodies on the contemporaneous GC. For example, these antibodies may mask the epitopes they target on antigens displayed on FDCs, thus leading to the evolution of higher-affinity GC antibodies that target these epitopes (43) and

may cause the GC to generate more diversity by promoting the evolution of B cells that target other normally subdominant epitopes (44, 45).

Data, Materials, and Software Availability. Code data have been deposited in GitHub (10.5281/zenodo.6399267) (46). Previously published data were used for this work (https://doi.org/10.1038/s41586-021-04060-7).

ACKNOWLEDGMENTS. M.V.B. was supported by National Institutes of Health grant no. U19AI057229; M.V.B. and A.K.C. were supported by the Ragon Institute of Massachusetts General Hospital, Massachusetts Institute of Technology, and Harvard; and M.C.N. is an HHMI investigator.

Author affiliations: [a]Department of Chemical Engineering, Massachusetts Institute of Technology, Cambridge, MA 02139; [b]Laboratory of Molecular Immunology, The Rockefeller University, New York, NY 10065; [c]HHMI; [d]Department of Physics, Massachusetts Institute of Technology, Cambridge, MA 02139; [e]Department of Chemistry, Massachusetts Institute of Technology, Cambridge, MA 02139; [f]Institute for Medical Engineering & Science, Massachusetts Institute of Technology, Cambridge, MA 02139; and [g]Ragon Institute of Massachusetts General Hospital, Massachusetts Institute of Technology and Harvard, Cambridge, MA 02139

1. C. A. Janeway, P. Travers, M. Walport, D. J. Capra, *Immunobiology* (New York: Garland Science, 2001).
2. G. D. Victora, M. C. Nussenzweig, Germinal centers. *Annu. Rev. Immunol.* **30**, 429–457 (2012).
3. M. Oprea, A. S. Perelson, Somatic mutation leads to efficient affinity maturation when centrocytes recycle back to centroblasts. *J. Immunol.* **158**, 5155–5162 (1997).
4. G. D. Victora *et al.*, Germinal center dynamics revealed by multiphoton microscopy with a photoactivatable fluorescent reporter. *Cell* **143**, 592–605 (2010).
5. H. N. Eisen, G. W. Siskind, Variations in affinities of antibodies during the immune response. *Biochemistry* **3**, 996–1008 (1964).
6. I. Moran, A. K. Grootveld, A. Nguyen, T. G. Phan, Subcapsular sinus macrophages: The seat of innate and adaptive memory in murine lymph nodes. *Trends Immunol.* **40**, 35–48 (2019).
7. L. A. Steiner, H. N. Eisen, The relative affinity of antibodies synthesized in the secondary response. *J. Exp. Med.* **126**, 1185–1205 (1967).
8. L. Mesin *et al.*, Restricted clonality and limited germinal center reentry characterize memory B cell reactivation by boosting. *Cell* **180**, 92–106.e11 (2020).
9. M. J. Shlomchik, Do memory B cells form secondary germinal centers? Yes and no. *Cold Spring Harb. Perspect. Biol.* **10**, a029405 (2018).
10. K. A. Pape, M. K. Jenkins, Do memory B cells form secondary germinal centers? It depends. *Cold Spring Harb. Perspect. Biol.* **10**, a029116 (2018).
11. T. A. Schwickert *et al.*, A dynamic T cell-limited checkpoint regulates affinity-dependent B cell entry into the germinal center. *J. Exp. Med.* **208**, 1243–1252 (2011).
12. T. G. Phan, I. Grigorova, T. Okada, J. G. Cyster, Subcapsular encounter and complement-dependent transport of immune complexes by lymph node B cells. *Nat. Immunol.* **8**, 992–1000 (2007).
13. T. Junt *et al.*, Subcapsular sinus macrophages in lymph nodes clear lymph-borne viruses and present them to antiviral B cells. *Nature* **450**, 110–114 (2007).
14. Y. R. Carrasco, F. D. Batista, B cells acquire particulate antigen in a macrophage-rich area at the boundary between the follicle and the subcapsular sinus of the lymph node. *Immunity* **27**, 160–171 (2007).
15. J. G. Cyster, B cell follicles and antigen encounters of the third kind. *Nat. Immunol.* **11**, 989–996 (2010).
16. I. Moran *et al.*, Memory B cells are reactivated in subcapsular proliferative foci of lymph nodes. *Nat. Commun.* **9**, 3372 (2018).
17. C. Viant *et al.*, Antibody affinity shapes the choice between memory and germinal center B cell fates. *Cell* **183**, 1298–1311.e11 (2020).
18. A. Amitai *et al.*, Defining and manipulating B cell immunodominance hierarchies to elicit broadly neutralizing antibody responses against influenza virus. *Cell Syst.* **11**, 573–588.e9 (2020).
19. A. Amitai, A. K. Chakraborty, M. Kardar, The low spike density of HIV may have evolved because of the effects of T helper cell depletion on affinity maturation. *PLOS Comput. Biol.* **14**, e1006408 (2018).
20. M. D. S. Kumar, M. M. Gromiha, PINT: Protein-protein interactions thermodynamic database. *Nucleic Acids Res.* **34**, D195–D198 (2006).
21. J. Zhang, E. I. Shakhnovich, Optimality of mutation and selection in germinal centers. *PLOS Comput. Biol.* **6**, e1000800 (2010).
22. L. Mesin, J. Ersching, G. D. Victora, Germinal center B cell dynamics. *Immunity* **45**, 471–482 (2016).
23. MathWorks, copularnd. https://www.mathworks.com/help/stats/copularnd.html. Accessed 17 August 2022.
24. D. D. Jones, J. R. Wilmore, D. Allman, Cellular dynamics of memory B cell populations: IgM+ and IgG+ memory B cells persist indefinitely as quiescent cells. *J. Immunol.* **195**, 4753–4759 (2015).
25. S. M. Anderson, L. G. Hannum, M. J. Shlomchik, Cutting edge: Memory B cell survival and function in the absence of secreted antibody and immune complexes on follicular dendritic cells. *J. Immunol.* **176**, 4515–4519 (2006).
26. A. Cho *et al.*, Anti-SARS-CoV-2 receptor-binding domain antibody evolution after mRNA vaccination. *Nature* **600**, 517–522 (2021).
27. W. E. Purtha, T. F. Tedder, S. Johnson, D. Bhattacharya, M. S. Diamond, Memory B cells, but not long-lived plasma cells, possess antigen specificities for viral escape mutants. *J. Exp. Med.* **208**, 2599–2606 (2011).
28. R. Wong *et al.*, Affinity-restricted memory B cells dominate recall responses to heterologous flaviviruses. *Immunity* **53**, 1078–1094.e7 (2020).
29. A. Mayer, V. Balasubramanian, A. M. Walczak, T. Mora, How a well-adapting immune system remembers. *Proc. Natl. Acad. Sci. U.S.A.* **116**, 8815–8823 (2019).
30. A. Mayer, V. Balasubramanian, T. Mora, A. M. Walczak, How a well-adapted immune system is organized. *Proc. Natl. Acad. Sci. U.S.A.* **112**, 5950–5955 (2015).
31. A. S. Perelson, G. F. Oster, Theoretical studies of clonal selection: Minimal antibody repertoire size and reliability of self-non-self discrimination. *J. Theor. Biol.* **81**, 645–670 (1979).
32. A. Gao *et al.*, Evolution of weak cooperative interactions for biological specificity. *Proc. Natl. Acad. Sci. U.S.A.* **115**, E11053–E11060 (2018).
33. J. S. Shaffer, P. L. Moore, M. Kardar, A. K. Chakraborty, Optimal immunization cocktails can promote induction of broadly neutralizing Abs against highly mutable pathogens. *Proc. Natl. Acad. Sci. U.S.A.* **113**, E7039–E7048 (2016).
34. M. J. Shlomchik, F. Weisel, Germinal center selection and the development of memory B and plasma cells. *Immunol. Rev.* **247**, 52–63 (2012).
35. V. Chardès, M. Vergassola, A. M. Walczak, T. Mora, Affinity maturation for an optimal balance between long-term immune coverage and short-term resource constraints. *Proc. Natl. Acad. Sci. U.S.A.* **119**, e2113512119 (2022).
36. O. H. Schnaack, A. Nourmohammad, Optimal evolutionary decision-making to store immune memory. *eLife* **10**, e61346 (2021).
37. F. J. Weisel, G. V. Zuccarino-Catania, M. Chikina, M. J. Shlomchik, A temporal switch in the germinal center determines differential output of memory B and plasma cells. *Immunity* **44**, 116–130 (2016).
38. T. G. Phan *et al.*, High affinity germinal center B cells are actively selected into the plasma cell compartment. *J. Exp. Med.* **203**, 2419–2424 (2006).
39. H. N. Eisen, Affinity enhancement of antibodies: How low-affinity antibodies produced early in immune responses are followed by high-affinity antibodies later and in memory B-cell responses. *Cancer Immunol. Res.* **2**, 381–392 (2014).
40. R. K. Abbott *et al.*, Precursor frequency and affinity determine B cell competitive fitness in germinal centers, tested with germline-targeting HIV vaccine immunogens. *Immunity* **48**, 133–146.e6 (2018).
41. P. Dosenovic *et al.*, Anti-HIV-1 B cell responses are dependent on B cell precursor frequency and antigen-binding affinity. *Proc. Natl. Acad. Sci. U.S.A.* **115**, 4743–4748 (2018).
42. R. K. Tennant, B. Holzer, J. Love, E. Tchilian, H. N. White, Higher levels of B-cell mutation in the early germinal centres of an inefficient secondary antibody response to a variant influenza haemagglutinin. *Immunology* **157**, 86–91 (2019).
43. Y. Zhang *et al.*, Germinal center B cells govern their own fate via antibody feedback. *J. Exp. Med.* **210**, 457–464 (2013).
44. J. J. E. Bergström, H. Xu, B. Heyman, Epitope-specific suppression of IgG responses by passively administered specific IgG: Evidence of epitope masking. *Front. Immunol.* **8**, 238 (2017).
45. M. Meyer-Hermann, Injection of antibodies against immunodominant epitopes tunes germinal centers to generate broadly neutralizing antibodies. *Cell Rep.* **29**, 1066–1073.e5 (2019).
46. M. V. Beek, M. C. Nussenzweig, A. K. Chakraborty, Two complementary features of humoral immune memory confer protection against the same or variant antigens. GitHub. https://zenodo.org/record/6399267#.YwOj13ZBy3A. Deposited 30 March 2022.